

Response of organic aerosol characteristics to emission reduction in Yangtze River Delta region

Jinbo Wang^{1,2}, Jiaping Wang (✉)^{1,2,3}, Wei Nie^{1,2,3}, Xuguang Chi^{1,2,3}, Dafeng Ge^{1,2}, Caijun Zhu^{1,2}, Lei Wang^{1,2,3}, Yuanyuan Li^{1,2}, Xin Huang^{1,2}, Ximeng Qi^{1,2,3}, Yuxuan Zhang^{1,2,3}, Tengyu Liu^{1,2,3}, Aijun Ding^{1,2,3}

¹ Joint International Research Laboratory of Atmospheric and Earth System Sciences, School of Atmospheric Sciences, Nanjing University, Nanjing 210023, China

² Jiangsu Provincial Collaborative Innovation Center of Climate Change, Nanjing 210023, China

³ National Observation and Research Station for Atmospheric Processes and Environmental Change in Yangtze River Delta, Nanjing 210023, China

HIGHLIGHTS

- The emission reduction causes significant change in organic aerosol composition.
- The atmospheric oxidizing capacity improved during emission reduction.
- The mixed oxygenated organic aerosol contributed higher during emission reduction.

ARTICLE INFO

Article history:

Received 26 December 2022

Revised 27 February 2023

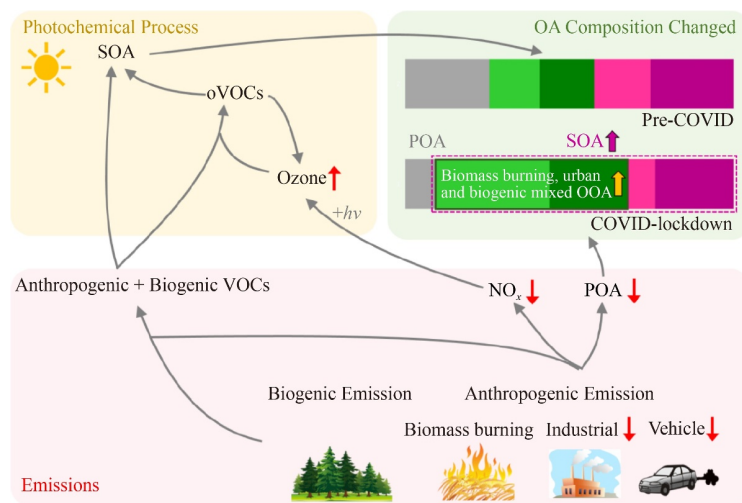
Accepted 7 March 2023

Available online 15 April 2023

Keywords:

Emission control
Secondary organic aerosol
Atmospheric oxidizing capacity
Holiday effects
COVID-19 lockdown

GRAPHIC ABSTRACT



ABSTRACT

Organic aerosol (OA) is a major component of atmospheric particulate matter (PM) with complex composition and formation processes influenced by various factors. Emission reduction can alter both precursors and oxidants which further affects secondary OA formation. Here we provide an observational analysis of secondary OA (SOA) variation properties in Yangtze River Delta (YRD) of eastern China in response to large scale of emission reduction during Chinese New Year (CNY) holidays from 2015 to 2020, and the COVID-19 pandemic period from January to March, 2020. We found a 17% increase of SOA proportion during the COVID lockdown. The relative enrichment of SOA is also found during multi-year CNY holidays with dramatic reduction of anthropogenic emissions. Two types of oxygenated OA (OOA) influenced by mixed emissions and SOA formation were found to be the dominant components during the lockdown in YRD region. Our results highlight that these emission-reduction-induced changes in organic aerosol need to be considered in the future to optimize air pollution control measures.

© Higher Education Press 2023

1 Introduction

Organic aerosol (OA) is one of the main components of

atmospheric particulate matter (PM) which has significant impacts on air quality, public health and climate (IPCC, 2021). OA has multiple sources and complex evolution in the atmosphere (Jimenez et al., 2009), and is usually categorized as primary OA (POA) and secondary OA (SOA) (Zhang et al., 2011). POA is emitted directly, and SOA is formed from the oxidation of volatile organic compounds (VOCs) (Kanakidou et al., 2005). The formation of SOA is related to a series of physical processes and chemical reactions (Aiken et al., 2008) which is affected by various factors, e.g., precursor concentrations, atmospheric oxidation capacity, and meteorological conditions (Donahue et al., 2006; Hennigan et al., 2009; Kim et al., 2018). There are many precursors of SOA (e.g., α -pinene, isoprene, toluene) which can react with oxidants, e.g., hydroxyl radical ($\cdot\text{OH}$), nitrate radical (NO_3), ozone (O_3), and hydrogen peroxide (H_2O_2) (Chhabra et al., 2011). SOA evolves continuously from less oxidized (LO) to more oxidized (MO) influenced by photochemical activities in the atmosphere (Ng et al., 2010; 2011; Zhang et al., 2011). Less or highly oxygenated organic molecules (OOM or HOM) may also contribute a significant fraction to SOA production (Ehn et al., 2014; Liu et al., 2021b; Zhao et al., 2021; Nie et al., 2022).

The change of anthropogenic emission alters the level of both precursors and oxidants which can influence secondary aerosol formation widely (Ding et al., 2019; Zhang and Geng, 2019; Zhang et al., 2019; Cai et al., 2022). Understanding the response of SOA to the change of pollutant emission is essential for optimizing the air pollution control strategies in the future, especially in the regions strongly affected by human activities. As strict lockdown measures to restrain the spread of coronavirus disease (COVID-19) after Chinese New Year (CNY) in 2020, COVID-lockdown can be considered as a "controlled experiment" to investigate the responses of air pollution to the large-scale forced emission reduction (Shi and Brasseur, 2020; Laughner et al., 2021; Liu et al., 2021a; Hu et al., 2022). Yet despite large reductions of primary pollutant (e.g., NO_2) in China (Bauwens et al., 2020), there were still several haze episodes (Sun et al., 2020b; Huang et al., 2021). Besides the COVID lockdown, the emission reduction of anthropogenic activity (Zhang et al., 2015a; Li et al., 2019; Yang et al., 2020), changes of aerosol composition (Kong et al., 2015; Zhao et al., 2017) and dominant role of secondary aerosol formation were also observed during the public holiday and anniversary (Lin et al., 2020; Sun et al., 2020b; Wang et al., 2021; Xu et al., 2022; Zhou et al., 2022b), which indicates that controlling local primary source emissions might have a limited effect on improving air quality in some megacities (Jiang et al., 2015). Hence, the weeklong CNY holiday can be considered as a similar condition with a nationwide emission reduction, providing us ideal experiments to explore the impacts of emission reduction on secondary aerosol formation.

OA is the most abundant component of PM in eastern

China (Wang et al., 2016; Zheng et al., 2016; Li et al., 2017b; Shang et al., 2021). The POA and SOA are often referred to HOA (hydrocarbon-like OA) and OOA (oxygenated OA), respectively in studies using aerosol mass spectrometry (Zhang et al., 2005). POA is closely related to emission sources, like vehicles (Ho et al., 2022), biomass burning (BBOA) and coal combustion (CCOA) (Li et al., 2017a; Sun et al., 2020a). POA has been observed widely in YRD which is one of the most-urbanized regions in China (Ye et al., 2017), and biomass burning plays an important role in the emission of POA (Zhang et al., 2015b). BBOA and biomass/biofuel burning-containing particles increased significantly during the haze events (Wang et al., 2014; Zhang et al., 2015d). In YRD, OOA dominates total OA (Li et al., 2017b), water-soluble OA (Ge et al., 2017) and black-carbon-containing particles (Cui et al., 2022) resulting from the substantial formation of secondary organic aerosols (Xu et al., 2019a) which is associated with aqueous-phase processing and photochemical oxidation (Huang et al., 2020) and greatly affected by summery semi-volatile organic compounds (Yu et al., 2021). Furthermore, environment condition including low wind speed, high relative humidity and O_3 can also favor OOA production and accumulation (Xu et al., 2019a; Wang et al., 2022a). OOA has clear seasonal variation in YRD (Huang et al., 2013; Zhao et al., 2020). The MO-OOA associates to nitrate closely due to regional transport (Sun et al., 2020a) in winter, while the low-volatile MO-OOA correlates more to sulfate than nitrate and has no positive correlations with relative humidity in spring, revealing a dominant role of photochemical oxidation (Wang et al., 2016). Semi-volatile LO-OOA relates to nitrate and shows a negative correlation with air temperature in spring of YRD, suggesting that the variations of them are driven by thermodynamic equilibria and gas-to-particle partitioning. The MO-OOA and low-volatility OOA increased sharply on haze days (Zhang et al., 2015c; Zhang et al., 2015d), indicating that secondary formation of carbonaceous aerosol contributed significantly to pollution (Hu et al., 2018; Wang et al., 2022b).

Considering the various measures to control air pollution and their complex influences on atmospheric chemistry, here we select typical emission reduction periods to investigate the response of atmospheric aerosols to primary emission change. Based on field observation and analysis, we demonstrate the change of major gaseous pollutants under emission reduction and their impacts on organic aerosol composition in YRD.

2 Materials and methods

2.1 Sampling site and measurements

The field observations were conducted from 1 January to

12 March 2020 at the Station for Observing Regional Processes of the Earth System (SORPES), located in the north-east Nanjing (118°57'10"E, 32°07'14"N). As the suburban site in Nanjing, The SORPES station has been considered as a regional background station in the YRD region because it is generally upwind from the city center and downwind of densely populated city clusters including several megacities (Ding et al., 2013b). More information about the SORPES station has been provided in previous studies (Ding et al., 2016a). The entire observation was classified into three stages: normal stage (Pre-COVID), lockdown stage (COVID-lockdown), and after-lockdown stage (Post-COVID) (Fig. S6), according to the schedule of COVID control regulation adopted by the government. The new-year days during the CNY (i.e., 24–25 January) was excluded because of possible firework effects on observation for COVID-lockdown. The observation for CNY from 2015 to 2020 was also classified into three stages: pre-CNY (the two weeks before the CNY), CNY (one week starting from CNY) and post-CNY (the two weeks after the CNY week).

The soot particle aerosol mass spectrometer (SP-AMS, Aerodyne Inc., USA) was used to measure non-refractory submicron aerosol composition (NR-PM₁) (Onasch et al., 2012; Massoli et al., 2015). The online measurement was performed in laser-off mode. PM_{2.5} mass concentration was measured by the online analyzer (Model 5030 SHARP, Thermo Instruments, USA). O₃, carbon monoxide (CO), nitric oxide (NO), nitrogen oxides (NO_x), sulfur dioxide (SO₂) and total reactive nitrogen (NO_y) were measured by online analyzers (TEI 49i, 48i, 42i, 42i, 43i, and 42iY, Thermo Instruments, USA). In addition, an atmospheric heavy metal online analyzer (EHM-X200, Tianrui Instrument, China) and an organic and elemental carbon (OC-EC) analyzer (Sunset Laboratory, USA) also measured simultaneously. Detailed description of above measurements was given in previous works (Ding et al., 2013a; Virkkula et al., 2015; Qi et al., 2018; Wang et al., 2018; Liu et al., 2019; Chen et al., 2021; Yang et al., 2021). Observation database of O₃ and NO₂ in different sites over China was obtained from the China National Urban Air Quality Real-time Publishing Platform supported by Ministry of Ecology and Environment.

2.2 Data processing and trajectory calculation

The SP-AMS data was processed by the standard ToF-AMS data analysis software packages (SQUIRREL version v1.60P and PIKA v1.20P). The SP-AMS operated in the common environment, so the typical collection efficiency (CE) value of 0.5 was valid and used in the study (Canagaratna et al., 2007). Ionization efficiency (IE) calibrations were done by sampling monodispersed 300 nm dried pure ammonium nitrate particles selected with a differential mobility analyzer (DMA, model 3081, TSI Inc., USA) into AMS. IE values were adjusted regu-

larly according to the periodical mass-based calibration. The relative IE (RIE) for OA, sulfate and ammonium is 1.4, 1.2 and 4.0, which was set as default values. Based on previous AMS measurements in the laboratory or ambient, the RIE does not have significant change and still approaches the default RIE in the sampling site located at the typical urbanized region (Canagaratna et al., 2007; Jimenez et al., 2016).

The components of OA were determined by positive matrix factorization (PMF) using PMF Evaluation Tool version 3.04A. We conducted PMF analysis on the organic high-resolution mass spectra (HRMS) following the method described in Ulbrich et al., (2009). Only ions that charge-to-mass ratio below 120 were considered. Five OA factors were identified as HOA, MOA (mixed OA), aged MOA, LO-OOA, and MO-OOA using PMF. The first factor is HOA (hydrocarbon-like OA) because it has significantly high signal of C₄H₇⁺ and C₄H₉⁺ (Fig. S1) and its variation correlates well with BC which is a primary pollutant (Fig. S2). HOA has been thought as a surrogate for primary combustion OA emitted massively by vehicle in city (Zhang et al., 2005). Other four factors are OOA which have higher signal of CO₂⁺ or CHO⁺. The second and third factors are named as MOA (mixed OA) and aged MOA, respectively. The fourth and fifth factors are more aged SOA (less oxidized oxygenated OA, LO-OOA and more oxidized oxygenated OA, MO-OOA). More detailed explanation about identification of these factors is provided in the result part and the Supplementary material (SI).

The 72 h backward trajectories were calculated and clustered using the Hybrid Single-Particle Lagrangian Integrated Trajectory (HYSPLIT) model (Stein et al., 2015). We calculated backward trajectories and distribution of the surface probability of the simulated air mass following the methods in Ding et al., (2013a; 2013c) and Sun et al., (2020a). The airmass initialized at an altitude of 100 m.

3 Results

Figure 1 presents the comparison of OC/EC ratio before, during and after CNY holiday in six years (from 2015 to 2020), in which a significantly higher value of OC/EC can be observed during holiday in almost all years compared with the periods before and after the holiday. OC/EC ratio increased by 30% to 100% in CNY holiday in different years, showing a relative enrichment of organic carbon. At the same time, NO_x decreased dramatically during CNY holiday (Fig. S7). Secondary OC (SOC) also showed higher concentration during CNY in some years (Fig. S8). Since OC/EC can be considered as an indicator of the level of secondary OA formation, increased OC/EC and SOC imply enhanced secondary formation of organic components during holiday in YRD

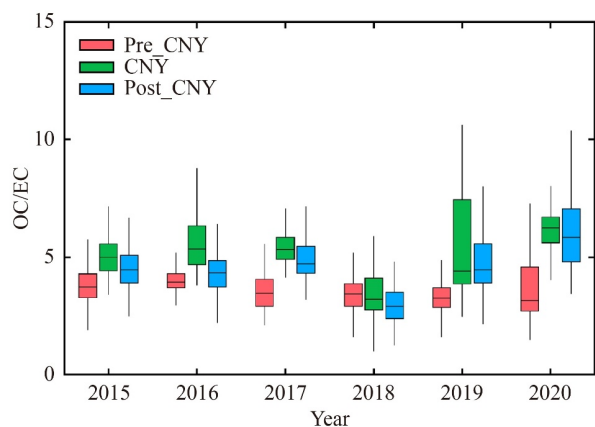


Fig. 1 Comparison of OC/EC during different periods (before CNY, during CNY and after CNY) around Chinese New Year from 2015 to 2020. Box plots represent the 25th and 75th percentiles and the whiskers stand for maximum and minimum values.

(Turpin and Huntzicker, 1995; Cheng et al., 2014; Feng et al., 2022).

Besides carbonaceous aerosol, we also analyzed the change in O_3 and NO_2 around the CNY in YRD and other regions of China (shown in Fig. S3 and Fig. 2). The ΔO_3 and ΔNO_2 are defined by the difference between each two stages (marked in each subplot in Fig. 2). Looking into O_3 concentration, it substantially increased at most of the sites in China during holiday (Figs. 2(a) and 2(c)). The regions with higher ΔO_3 (greater than 20 ppb), i.e. from North China Plain to YRD, corresponded well to massive NO_2 reduction area (Figs. S3a and S3c). After holiday, O_3 concentration suddenly dropped at most sites. The variation of O_3 and NO_2 during holiday is consistent with COVID lockdown period, which experienced similar emission reduction. Model results (Fig. S4) for eastern China shows that lower NO_x emission resulted in O_3 increasing due to influence of VOC-limited regime, which was mentioned by previous study in YRD (Xu et al., 2017). As a result, atmospheric oxidizing capacity could enhance (Huang et al., 2021), which may further affect secondary aerosol formation.

To further investigate OA characteristics in response to intense emission reduction, we selected the COVID lockdown period to conduct field observation using aerosol mass spectrometer. The overview of meteorological conditions and air pollutant concentrations during entire measurement period is presented in Fig. 3. Total aerosol concentration was high in winter without lockdown due to the adverse diffusion conditions caused by lower planetary boundary layer (Ding et al., 2016b), fuel combustion for residential heating (Wang et al., 2019), and regional transport of air pollutants (Sun et al., 2020a). Most of pollutants like nitrogen oxides (NO_x), black carbon (BC), and other aerosol species decreased dramatically during the COVID-lockdown under the influence of emission reduction. The mixing ratio of O_3

increased during lockdown period. Weakened NO-titration effect caused by the sharp decrease of NO emitted from traffic (Wu et al., 2019) is a possible reason for the rise of O_3 since the site is generally in VOC-limited regime (Xu et al., 2017) as Fig. S4 shown. In addition, the air temperature rose slightly from pre-COVID to post-COVID stage (mean values were 4.6, 7.3, and 10.5 °C, respectively) together with the decrease of relative humidity (mean values were 75.8%, 63.9% and 60.9%).

The comparison of aerosol chemical composition including organics (Org), sulfate (SO_4^{2-}), nitrate (NO_3^-), ammonium (NH_4^+) and chloride (Cl^-) before and during lockdown is shown in Fig. 3. Nitrate was the dominant component before COVID accounting for 39% in NR_PM_{10} , followed by OA. This is consistent to the tendency that the fraction of fine PM nitrate is increasing in YRD in recent years (Ding et al., 2019; Zhou et al., 2022a). However, nitrate dropped significantly due to the sharp decrease of its precursor during the lockdown. Meanwhile, OA took up the largest proportion (37%) of total aerosol mass. The concentration of all OA factors decreased during the lockdown episode. However, the chemical composition of OA changed significantly from Pre-COVID to COVID-lock period. HOA took up the highest proportion (26%) in OA during Pre-COVID, while it decreased dramatically during COVID-lock due to the reduction of anthropogenic emission. MO-OOA mass fraction was relatively stable (around 25%) in the entire sampling period. Compared with MO-OOA, the contribution of MOA and aged MOA boosted. The MOA and aged MOA became the dominant OA components (with mass fraction of 35% and 24%, respectively) during the COVID-lockdown.

As mentioned above, two special types of OOA were found during the measurement period which were identified as MOA and aged MOA, respectively. It is noticed that the both factors correlate well to $C_2H_4O_2^+$ and $C_5H_6O^+$ concurrently (Fig. 4) at all three stages, although these two ions indicate different OA sources, i.e., biomass burning (BB) and isoprene epoxydiols-derived secondary organic aerosol (IEPOX-SOA) (Aiken et al., 2009; Hu et al., 2015). The MOA and aged MOA mass spectrum are similar ($r = 0.93$). The two factors might represent OOA influenced by biomass burning (Crippa et al., 2013; Zhang et al., 2015b) because they are similar to oxygenated BBOA (Fig. S1) and have lower fraction of $C_2H_4O_2^+$ signal than typical BBOA (Aiken et al., 2009). The signal of $C_5H_6O^+$ is also higher than atmospheric background level in the profile of these factors. Hence, they may also be influenced by biogenic emission (Xu et al., 2015; Shilling et al., 2018; Shrivastava et al., 2019), which needs further study. In addition, they may be the mixture of BBOA with OOA (Crippa et al., 2013) related to regional transport. OA from regional biomass burning (Hu et al., 2016; Li et al.,

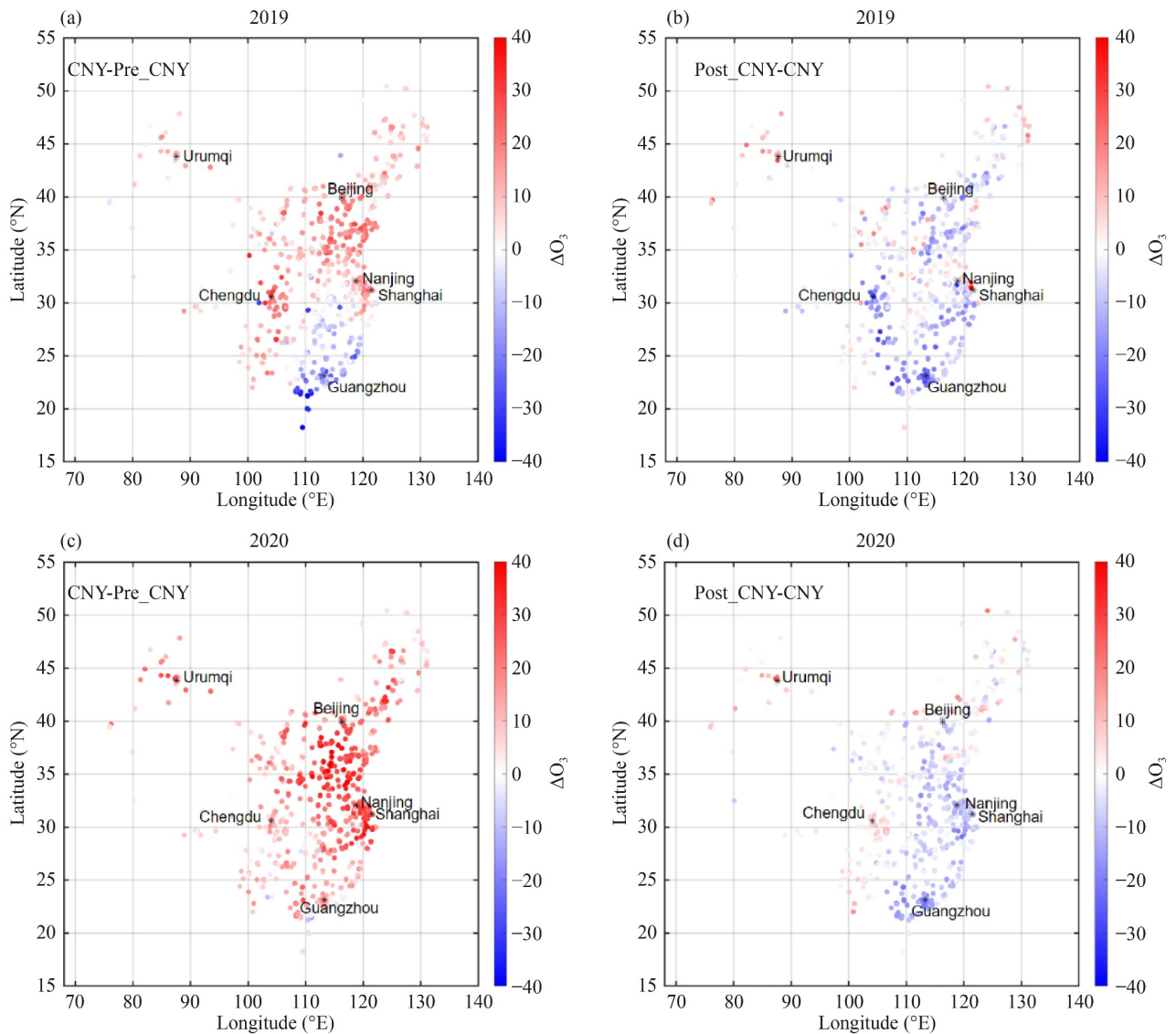


Fig. 2 Change of 8 h moving average of surface O_3 concentration before, during and after Chinese New Year (CNY) Holiday. The unit of O_3 is $\mu\text{g}/\text{m}^3$. (a) and (c) the change of O_3 concentration during CNY holiday minus that before CNY holiday in 2019 and 2020, respectively; (b) and (d) the change of O_3 concentration after CNY holiday minus that during CNY holiday in 2019 and 2020, respectively. The underlying graph is reference grid for longitude and latitude, and not involved with coastline, boundary line or any other boundaries.

2018; Xu et al., 2019b; Huang et al., 2020; Li et al., 2021), biogenic emission (Fu et al., 2016; Wu et al., 2020; Xu et al., 2021) and other sources can mix well and reach the sampling site by air mass transport. The aged MOA contains relatively more oxygen and less hydrogen than MOA. The higher oxidation degree of aged MOA implies that aged MOA may stay in atmosphere longer than MOA with additional photochemical oxidizing process that makes the less oxidized component evolving into the more oxidized component (Jimenez et al., 2009; Huang et al., 2012).

Since MOA and aged MOA took up a high fraction in OA during the lockdown, we also compared OA composition in each type of air mass cluster before and

during lockdown to investigate the OA source and potential influence of regional transport. 72 h backward trajectories were calculated and clustered into six types of air masses (Fig. S5). The air masses from central and eastern YRD region, local area, and northern region are major contributors to the observation site. As presented in Fig. 5, HOA mass fraction decreased during lockdown in all three clusters, showing a large scale of primary emission reduction. Meanwhile, both MOA and aged MOA fractions exhibited a significant increase while LO-OA fraction dropped during lockdown. Since MOA and aged MOA have apparent BB signal, the increased proportion of these two factors indicates the enhanced impact of BB-related activities during the COVID-lock,



Fig. 3 Time series of hourly averaged gaseous pollutants, meteorological parameters, combustion aerosol and non-refractory aerosol species (Org, NO_3^- , SO_4^{2-} , NH_4^+ , Cl^-) from January to March in 2020. The pie charts present the average PM_{10} and organic aerosol (OA) composition during the pre-COVID and COVID-lockdown periods.

such as domestic heating by biomass (Mao et al., 2018), which was less affected by the lockdown. Besides, the isoprene concentration showed a much less decrease than primary emission pollutants such as NO_x , toluene, and EC (Fig. S6), higher fraction of MOA and aged MOA is also possibly affected by biogenic emissions. The fraction of MO-OOA decreased in local and YRD airmass in the lockdown period. However, MO-OOA took up a higher proportion in the airmass from the NCP, implying a relatively higher oxidation state of OOA in this regional transported air masses to the observation site during the lockdown.

To compare the changing degree of primary and secondary OA during the lockdown, the ratio of OOA during COVID-lock versus pre-COVID and that of HOA (following the method in Huang et al., (2021)) was presented in Fig. 6. It can be observed that the OOA decreased much less than HOA during COVID-lock. The ratio of ΔOOA during lockdown was much higher than ΔHOA in all types of clusters ($\Delta\text{OOA}/\Delta\text{HOA}_{\text{lock/pre}}$ larger than 150%), illustrating a generally enhancement of SOA formation compared to the large scale of primary emission reduction. The ratio of $\Delta\text{OOA}/\Delta\text{HOA}_{\text{lock/pre}}$ differed among different airmass. The Local airmass

presented the highest ratio of $\Delta\text{OOA}/\Delta\text{HOA}_{\text{lock/pre}}$, implying a substantial secondary formation of OA. This ratio was larger in the Northern airmass (~300%) than that in the YRD airmass (~200%) which provided further evidence that OA tend to get more aged during lockdown in northern part of China compared to the YRD region.

To further investigate the relative changes of secondary aerosol species over primary aerosols, the change ratio of OA/EC , NO_3^-/EC and $\text{SO}_4^{2-}/\text{EC}$ between COVID-lock and Pre-COVID period was calculated in each airmass cluster and the results are shown in Fig. 7. Overall, the change rate of OA/EC (0.16, 0.21 and 0.46) was all positive in the Local, YRD, and Northern airmasses, indicating the promoted secondary formation of OA in the lockdown period. The O_3 mixing ratio doubled during the COVID-lock. Such sharp O_3 enhancement induced by the drop of NO_x and weakened NO titration effect (Fig. S3 and S4) could be the major factor leading to promoted OA formation. The change ratio of sulfate was only positive in Northern airmass cluster during the lockdown. As for the period controlled by local and YRD airmass, the relative increase of organics is higher than that of sulfate and nitrate during the lockdown, implying a significant strengthened SOA formation. The nitrate

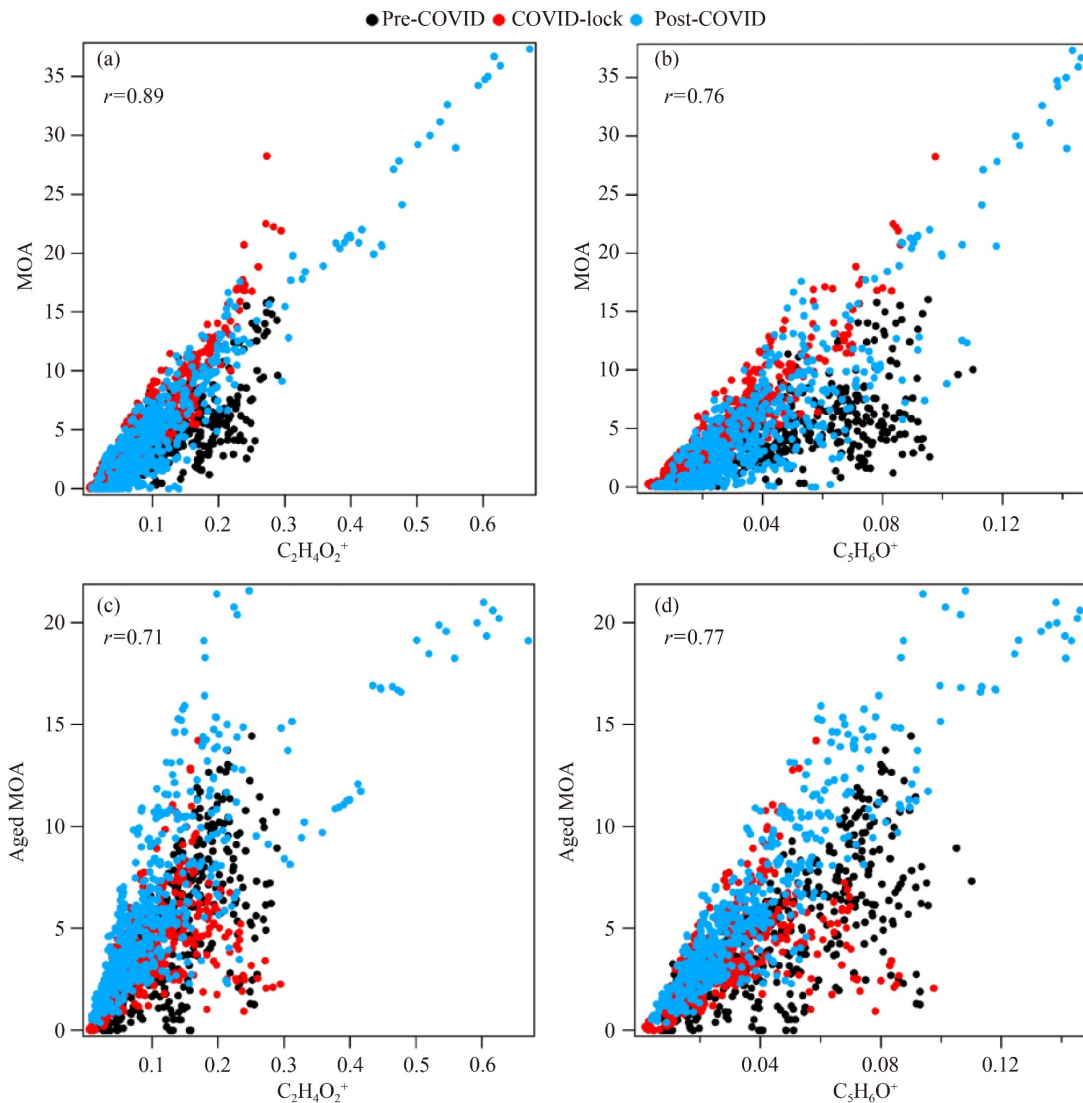


Fig. 4 Scatter plots of the mixed OA (MOA) and aged mixed OA (Aged MOA) vs. the $\text{C}_2\text{H}_4\text{O}_2^+$ and $\text{C}_5\text{H}_6\text{O}^+$ ions. The $\text{C}_2\text{H}_4\text{O}_2^+$ and $\text{C}_5\text{H}_6\text{O}^+$ ions are tracer ions of biomass burning and IEPOX-SOA respectively (Aiken et al., 2009; Hu et al., 2015). The “ r ” stands for the Pearson correlation coefficient. The colors of the points represent the observation periods. The units of OA factors and ions concentration are $\mu\text{g}/\text{m}^3$. (a) MOA mass concentration vs. $\text{C}_2\text{H}_4\text{O}_2^+$ mass concentration; (b) MOA mass concentration vs. $\text{C}_5\text{H}_6\text{O}^+$ mass concentration; (c) Aged MOA mass concentration vs. $\text{C}_2\text{H}_4\text{O}_2^+$ mass concentration; (d) Aged MOA mass concentration vs. $\text{C}_5\text{H}_6\text{O}^+$ mass concentration.

formation was suppressed in all three clusters during the lockdown caused by a dramatic decrease of anthropogenic NO_x emission from diminished transportation activities (Fig. S6).

4 Conclusions and implications

In this study, we investigated the characteristics and impact factors of organic aerosol in response to emission reductions in western YRD region. We observed a noticeable increase of OC/EC ratio during the CNY holidays, indicating a relative enrichment of secondary organic aerosol. The OC/EC ratio was higher than 5

during holidays in most years. Increased O_3 was found in majority of cities in China during the CNY holidays, especially from North China Plain to the YRD region. It implies that SOA formation might promote during holiday affected by O_3 boosting.

Further, we measured organic aerosol using SP-AMS and made analysis by PMF. Two types of mixed OOA factors were discovered which were related to both anthropogenic and biogenic emissions at the same time. With massive reduction of fossil fuel and vehicle emissions during the lockdown, MOA and aged MOA became the dominant components accounting for 59% of the total OA mass, which may be influenced by mixed sources including BB and regional transport of aged OA.

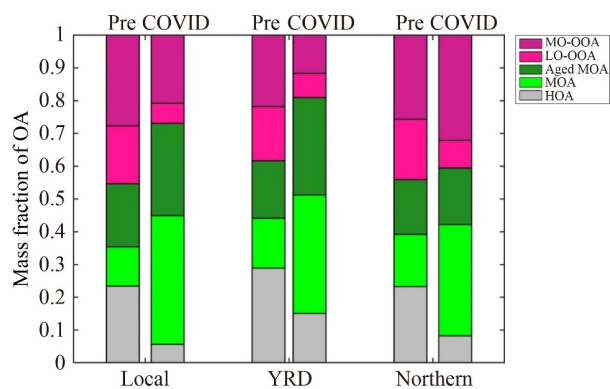


Fig. 5 The stacked bar plot of the mass fraction of five OA factors in different airmass clusters before and during the COVID lockdown. The airmass of different clusters is from local region, Yangtze River Delta (YRD), and northern region.

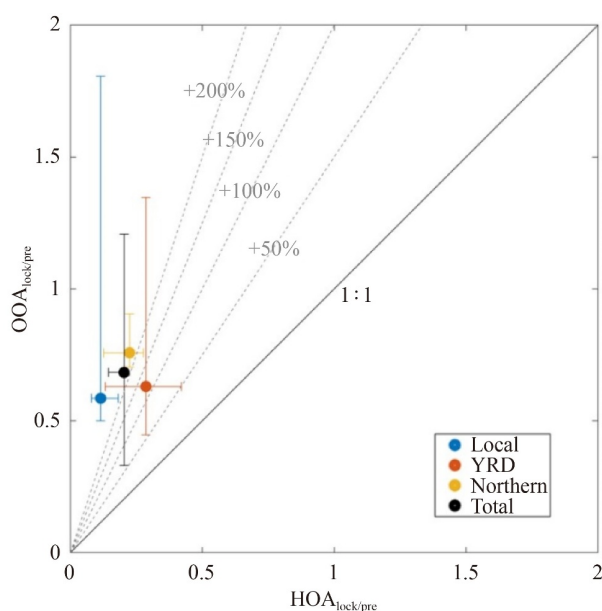


Fig. 6 The ratio of $OOA_{lock/pre}$ to OOA_{pre} (the mean OOA concentration during the COVID-lock versus the mean OOA concentration during the pre-COVID periods) as a function of the ratio of $HOA_{lock/pre}$ to HOA_{pre} (the mean HOA concentration during the COVID-lock versus the mean HOA concentration during the pre-COVID periods). The different points represent ratios in different airmass-transport condition, i.e., local, Yangtze River Delta regional (YRD) and northern airmass clusters. Horizontal error bars represent the range of $HOA_{lock-pre}$ quantile (tenth, median and ninetieth) ratio. Vertical error bars represent the range of $OOA_{lock-pre}$ quantile (tenth, median and ninetieth) ratio.

The less decrease in SOA and sharp increase in O_3 mixing ratio indicate rising atmospheric oxidation capacity to promote SOA formation during COVID-lock. Furthermore, SOA formation was stronger in airmass transported from the NCP compared to that from the YRD and local regions. Overall, our study provides an insight that organic aerosol composition changes

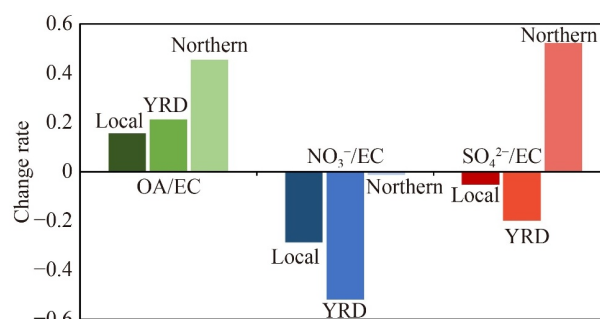


Fig. 7 Change ratio of OA, nitrate, and sulfate concentrations in the COVID-lock stage compared to the Pre-COVID stage. The shade of histogram represents the change ratio in different airmass-transport condition, i.e., local, Yangtze River Delta (YRD) regional and northern airmass clusters. The formula to calculate change ratio of species X is $(X_{lock} - X_{pre}) / X_{pre}$.

markedly in response to emission reduction scenarios including air quality control during large events, public holidays, and future emission reduction conditions. Therefore, this emission-reduction-induced changes of organic aerosol needs to be considered to optimize the pollution control measures in the future.

Acknowledgements This work is mainly supported by National Natural Science Foundation of China (No. 42005082). We would like to thank Wenjun Wu and Zheng Xu, who helped maintaining the instruments during the COVID-lock. Also, we thank Liwen Yang and Guangdong Niu for helping data management and thank Xiaolei Wang for sorting the air quality data from national data platform.

Electronic Supplementary Material Supplementary material is available in the online version of this article at <https://doi.org/10.1007/s11783-023-1714-0> and is accessible for authorized users.

References

- Aiken A C, Decarlo P F, Kroll J H, Worsnop D R, Huffman J A, Docherty K S, Ulbrich I M, Mohr C, Kimmel J R, Sueper D, et al. (2008). O/C and OM/OC ratios of primary, secondary, and ambient organic aerosols with high-resolution time-of-flight aerosol mass spectrometry. *Environmental Science & Technology*, 42(12): 4478–4485
- Aiken A C, Salcedo D, Cubison M J, Huffman J A, Decarlo P F, Ulbrich I M, Docherty K S, Sueper D, Kimmel J R, Worsnop D R, et al. (2009). Mexico City aerosol analysis during MILAGRO using high resolution aerosol mass spectrometry at the urban supersite (T0)—Part 1: Fine particle composition and organic source apportionment. *Atmospheric Chemistry and Physics*, 9(17): 6633–6653
- Bauwens M, Compornolle S, Stavrakou T, Muller J F, Gent J, Eskes H, Levelt P F, A R, Veeckind J P, Vlietinck J, Yu H, et al. (2020). Impact of coronavirus outbreak on NO_2 pollution assessed using TROPOMI and OMI observations. *Geophysical Research Letters*, 47(11): 2020GL087978
- Cai J, Wu C, Wang J D, Du W, Zheng F X, Hakala S M, Fan X L, Chu

- B W, Yao L, Feng Z M, et al. (2022). Influence of organic aerosol molecular composition on particle absorptive properties in autumn Beijing. *Atmospheric Chemistry and Physics*, 22(2): 1251–1269
- Canagaratna M R, Jayne J T, Jimenez J L, Allan J D, Alfarra M R, Zhang Q, Onasch T B, Drewnick F, Coe H, Middlebrook A, et al. (2007). Chemical and microphysical characterization of ambient aerosols with the aerodyne aerosol mass spectrometer. *Mass Spectrometry Reviews*, 26(2): 185–222
- Chen L D, Qi X M, Nie W, Wang J P, Xu Z, Wang T Y, Liu Y L, Shen Y C, Xu Z N, Kokkonen T V, et al. (2021). Cluster analysis of submicron particle number size distributions at the SORPES station in the Yangtze River Delta of East China. *Journal of Geophysical Research. Atmospheres*, 126(13): 2020JD034004
- Cheng Y, He K B, Duan F K, Du Z Y, Zheng M, Ma Y L (2014). Ambient organic carbon to elemental carbon ratios: influence of the thermal-optical temperature protocol and implications. *Science of the Total Environment*, 468–469: 1103–1111
- Chhabra P S, Ng N L, Canagaratna M R, Corrigan A L, Russell L M, Worsnop D R, Flagan R C, Seinfeld J H (2011). Elemental composition and oxidation of chamber organic aerosol. *Atmospheric Chemistry and Physics*, 11(17): 8827–8845
- Crippa M, Decarlo P F, Slowik J G, Mohr C, Heringa M F, Chirico R, Poulain L, Freutel F, Sciare J, Cozic J, et al. (2013). Wintertime aerosol chemical composition and source apportionment of the organic fraction in the metropolitan area of Paris. *Atmospheric Chemistry and Physics*, 13(2): 961–981
- Cui S J, Huang D D, Wu Y Z, Wang J F, Shen F Z, Xian J K, Zhang Y J, Wang H L, Huang C, Liao H, Ge X L (2022). Chemical properties, sources and size-resolved hygroscopicity of submicron black-carbon-containing aerosols in urban Shanghai. *Atmospheric Chemistry and Physics*, 22(12): 8073–8096
- Ding A, Nie W, Huang X, Chi X, Sun J, Kerminen V M, Xu Z, Guo W, Petaja T, Yang X, et al. (2016a). Long-term observation of air pollution-weather/climate interactions at the SORPES station: a review and outlook. *Frontiers of Environmental Science & Engineering*, 10(5): 15
- Ding A, Wang T, Fu C (2013a). Transport characteristics and origins of carbon monoxide and ozone in Hong Kong, South China. *Journal of Geophysical Research. Atmospheres*, 118(16): 9475–9488
- Ding A J, Fu C B, Yang X Q, Sun J N, Petaja T, Kerminen V M, Wang T, Xie Y, Herrmann E, Zheng L F, et al. (2013b). Intense atmospheric pollution modifies weather: a case of mixed biomass burning with fossil fuel combustion pollution in eastern China. *Atmospheric Chemistry and Physics*, 13(20): 10545–10554
- Ding A J, Fu C B, Yang X Q, Sun J N, Zheng L F, Xie Y N, Herrmann E, Nie W, Petaja T, Kerminen V M, et al. (2013c). Ozone and fine particle in the western Yangtze River Delta: an overview of 1 yr data at the SORPES station. *Atmospheric Chemistry and Physics*, 13(11): 5813–5830
- Ding A J, Huang X, Nie W, Chi X G, Xu Z, Zheng L F, Xu Z N, Xie Y N, Qi X M, Shen Y C, et al. (2019). Significant reduction of PM_{2.5} in eastern China due to regional-scale emission control: evidence from SORPES in 2011–2018. *Atmospheric Chemistry and Physics*, 19(18): 11791–11801
- Ding A J, Huang X, Nie W, Sun J N, Kerminen V M, Petaja T, Su H, Cheng Y F, Yang X Q, Wang M H, et al. (2016b). Enhanced haze pollution by black carbon in megacities in China. *Geophysical Research Letters*, 43(6): 2873–2879
- Donahue N M, Robinson A L, Stanier C O, Pandis S N (2006). Coupled partitioning, dilution, and chemical aging of semivolatile organics. *Environmental Science & Technology*, 40(8): 2635–2643
- Ehn M, Thornton J A, Kleist E, Sipila M, Junninen H, Pullinen I, Springer M, Rubach F, Tillmann R, Lee B, et al. (2014). A large source of low-volatility secondary organic aerosol. *Nature*, 506(7489): 476–479
- Feng Z M, Zheng F X, Liu Y C, Fan X L, Yan C, Zhang Y S, Daellenbach K R, Bianchi F, Petaja T, Kulmala M, et al. (2022). Evolution of organic carbon during COVID-19 lockdown period: possible contribution of nocturnal chemistry. *Science of the Total Environment*, 808: 152191
- Fu P Q, Zhuang G S, Sun Y L, Wang Q Z, Chen J, Ren L J, Yang F, Wang Z F, Pan X L, Li X D, et al. (2016). Molecular markers of biomass burning, fungal spores and biogenic SOA in the Taklimakan desert aerosols. *Atmospheric Environment*, 130: 64–73
- Ge X L, Li L, Chen Y F, Chen H, Wu D, Wang J F, Xie X C, Ge S, Ye Z L, Xu J Z, et al. (2017). Aerosol characteristics and sources in Yangzhou, China resolved by offline aerosol mass spectrometry and other techniques. *Environmental Pollution*, 225: 74–85
- Hennigan C J, Bergin M H, Russell A G, Nenes A, Weber R J (2009). Gas/particle partitioning of water-soluble organic aerosol in Atlanta. *Atmospheric Chemistry and Physics*, 9(11): 3613–3628
- Ho C S, Peng J F, Yun U, Zhang Q J, Mao H J (2022). Impacts of methanol fuel on vehicular emissions: a review. *Frontiers of Environmental Science & Engineering*, 16(9): 121
- Hu R, Wang H L, Yin Y, Chen K, Zhu B, Zhang Z F, Kang H, Shen L J (2018). Mixing state of ambient aerosols during different fog-haze pollution episodes in the Yangtze River Delta, China. *Atmospheric Environment*, 178: 1–10
- Hu R L, Wang S X, Zheng H T, Zhao B, Liang C R, Chang X, Jiang Y Q, Yin R J, Jiang J K, Hao J M (2022). Variations and sources of organic aerosol in winter Beijing under markedly reduced anthropogenic activities during COVID-2019. *Environmental science & technology*, 56(11): 6956–6967
- Hu W W, Campuzano-Jost P, Palm B B, Day D A, Ortega A M, Hayes P L, Krechmer J E, Chen Q, Kuwata M, Liu Y J, et al. (2015). Characterization of a real-time tracer for isoprene epoxydiols-derived secondary organic aerosol (IEPOX-SOA) from aerosol mass spectrometer measurements. *Atmospheric Chemistry and Physics*, 15(20): 11807–11833
- Hu W W, Hu M, Hu W, Jimenez J L, Yuan B, Chen W T, Wang M, Wu Y S, Chen C, Wang Z B, et al. (2016). Chemical composition, sources, and aging process of submicron aerosols in Beijing: contrast between summer and winter. *Journal of Geophysical Research. Atmospheres*, 121(4): 1955–1977
- Huang D D, Kong L, Gao J, Lou S R, Qiao L P, Zhou M, Ma Y G, Zhu S H, Wang H L, Chen S Y, et al. (2020). Insights into the formation and properties of secondary organic aerosol at a background site in Yangtze River Delta region of China: aqueous-phase processing vs. photochemical oxidation. *Atmospheric Environment*, 239: 117716
- Huang X, Ding A J, Gao J, Zheng B, Zhou D R, Qi X M, Tang R, Wang J P, Ren C H, Nie W, et al. (2021). Enhanced secondary pollution offset reduction of primary emissions during COVID-19

- lockdown in China. *National Science Review*, 8(2): nwaal37
- Huang X F, He L Y, Xue L, Sun T L, Zeng L W, Gong Z H, Hu M, Zhu T (2012). Highly time-resolved chemical characterization of atmospheric fine particles during 2010 Shanghai World Expo. *Atmospheric Chemistry and Physics*, 12(11): 4897–4907
- Huang X F, Xue L, Tian X D, Shao W W, Sun T L, Gong Z H, Ju W W, Jiang B, Hu M, He L Y (2013). Highly time-resolved carbonaceous aerosol characterization in Yangtze River Delta of China: Composition, mixing state and secondary formation. *Atmospheric Environment*, 64: 200–207
- IPCC (2021). *Climate Change 2021*. Masson-Delmotte V, eds. The Physical Science Basis. Contribution of Working Group I to the Sixth Assessment Report of the Intergovernmental Panel on Climate Change. Cambridge University Press, Cambridge, United Kingdom and New York, NY, USA
- Jiang Q, Sun Y L, Wang Z, Yin Y (2015). Aerosol composition and sources during the Chinese Spring Festival: fireworks, secondary aerosol, and holiday effects. *Atmospheric Chemistry and Physics*, 15(11): 6023–6034
- Jimenez J L, Canagaratna M R, Donahue N M, Prevot A S H, Zhang Q, Kroll J H, Decarlo P F, Allan J D, Coe H, Ng N L, et al. (2009). Evolution of organic aerosols in the atmosphere. *Science*, 326(5959): 1525–1529
- Jimenez J L, Canagaratna M R, Drewnick F, Allan J D, Alfarra M R, Middlebrook A M, Slowik J G, Zhang Q, Coe H, Jayne J T, et al. (2016). Comment on “The effects of molecular weight and thermal decomposition on the sensitivity of a thermal desorption aerosol mass spectrometer”. *Aerosol Science and Technology*, 50(9): 1–15
- Kanakidou M, Seinfeld J H, Pandis S N, Barnes I, Dentener F J, Facchini M C, Van Dingenen R, Ervens B, Nenes A, Nielsen C J, et al. (2005). Organic aerosol and global climate modelling: a review. *Atmospheric Chemistry and Physics*, 5(4): 1053–1123
- Kim H, Zhang Q, Heo J (2018). Influence of intense secondary aerosol formation and long-range transport on aerosol chemistry and properties in the Seoul Metropolitan Area during spring time: results from KORUS-AQ. *Atmospheric Chemistry and Physics*, 18(10): 7149–7168
- Kong S F, Li L, Li X X, Yin Y, Chen K, Liu D T, Yuan L, Zhang Y J, Shan Y P, Ji Y Q (2015). The impacts of firework burning at the Chinese Spring Festival on air quality: insights of tracers, source evolution and aging processes. *Atmospheric Chemistry and Physics*, 15(4): 2167–2184
- Laughner J L, Neu J L, Schimel D, Wennberg P O, Barsanti K, Bowman K W, Chatterjee A, Croes B E, Fitzmaurice H L, Henze D K, et al. (2021). Societal shifts due to COVID-19 reveal large-scale complexities and feedbacks between atmospheric chemistry and climate change. *Proceedings of the National Academy of Sciences of the United States of America*, 118(46)
- Li H, Zhang Q, Zhang Q, Chen C, Wang L, Wei Z, Zhou S, Parworth C, Zheng B, Canonaco F, et al. (2017a). Wintertime aerosol chemistry and haze evolution in an extremely polluted city of the North China Plain: significant contribution from coal and biomass combustion. *Atmospheric Chemistry and Physics*, 17(7): 4751–4768
- Li H Y, Zhang Q, Jiang W Q, Collier S, Sun Y L, Zhang Q, He K B (2021). Characteristics and sources of water-soluble organic aerosol in a heavily polluted environment in Northern China. *Science of the Total Environment*, 758: 143970
- Li K, Li J L, Tong S R, Wang W G, Huang R J, Ge M F (2019). Characteristics of wintertime VOCs in suburban and urban Beijing: concentrations, emission ratios, and festival effects. *Atmospheric Chemistry and Physics*, 19(12): 8021–8036
- Li L J, Ren L J, Ren H, Yue S Y, Xie Q R, Zhao W Y, Kang M J, Li J, Wang Z F, Sun Y L, et al. (2018). Molecular characterization and seasonal variation in primary and secondary organic aerosols in Beijing, China. *Journal of Geophysical Research. Atmospheres*, 123(21): 12394–12412
- Li Y J, Sun Y, Zhang Q, Li X, Li M, Zhou Z, Chan C K (2017b). Real-time chemical characterization of atmospheric particulate matter in China: a review. *Atmospheric Environment*, 158: 270–304
- Lin C S, Huang R J, Xu W, Duan J, Zheng Y, Chen Q, Hu W W, Li Y J, Ni H Y, Wu Y F, Zhang R J, et al. (2020). Comprehensive source apportionment of submicron aerosol in Shijiazhuang, China: secondary aerosol formation and holiday effects. *ACS Earth & Space Chemistry*, 4(6): 947–957
- Liu L, Zhang J, Du R G, Teng X M, Hu R, Yuan Q, Tang S S, Ren C H, Huang X, Xu L, et al. (2021a). Chemistry of atmospheric fine particles during the COVID-19 pandemic in a megacity of eastern China. *Geophysical Research Letters*, 48(2): 2020GL091611
- Liu Y L, Nie W, Li Y Y, Ge D F, Liu C, Xu Z N, Chen L D, Wang T Y, Wang L, Sun P, et al. (2021b). Formation of condensable organic vapors from anthropogenic and biogenic volatile organic compounds (VOCs) is strongly perturbed by NO_x in eastern China. *Atmospheric Chemistry and Physics*, 21(19): 14789–14814
- Liu Y L, Nie W, Xu Z, Wang T Y, Wang R X, Li Y Y, Wang L, Chi X G, Ding A J (2019). Semi-quantitative understanding of source contribution to nitrous acid (HONO) based on 1 year of continuous observation at the SORPES station in eastern China. *Atmospheric Chemistry and Physics*, 19(20): 13289–13308
- Mao S D, Li J, Cheng Z N, Zhong G C, Li K C, Liu X, Zhang G (2018). Contribution of biomass burning to ambient particulate polycyclic aromatic hydrocarbons at a regional background site in east China. *Environmental Science & Technology Letters*, 5(2): 56–61
- Massoli P, Onasch T B, Cappa C D, Nuaman I, Hakala J, Hayden K, Li S M, Sueper D T, Bates T S, Quinn P K, et al. (2015). Characterization of black carbon-containing particles from soot particle aerosol mass spectrometer measurements on the R/V Atlantis during CalNex 2010. *Journal of Geophysical Research. Atmospheres*, 120(6): 2575–2593
- Ng N L, Canagaratna M R, Jimenez J L, Chhabra P S, Seinfeld J H, Worsnop D R (2011). Changes in organic aerosol composition with aging inferred from aerosol mass spectra. *Atmospheric Chemistry and Physics*, 11(13): 6465–6474
- Ng N L, Canagaratna M R, Zhang Q, Jimenez J L, Tian J, Ulbrich I M, Kroll J H, Docherty K S, Chhabra P S, Bahreini R, et al. (2010). Organic aerosol components observed in Northern Hemispheric datasets from Aerosol Mass Spectrometry. *Atmospheric Chemistry and Physics*, 10(10): 4625–4641
- Nie W, Yan C, Huang D D, Wang Z, Liu Y, Qiao X, Guo Y, Tian L, Zheng P, Xu Z, et al. (2022). Secondary organic aerosol formed by condensing anthropogenic vapours over China’s megacities. *Nature*

- Geoscience, 15: 255–261
- Onasch T B, Trimborn A, Fortner E C, Jayne J T, Kok G L, Williams L R, Davidovits P, Worsnop D R (2012). Soot particle Aerosol Mass Spectrometer: development, validation, and initial application. *Aerosol Science and Technology*, 46(7): 804–817
- Qi X M, Ding A J, Roldin P, Xu Z N, Zhou P T, Sarnela N, Nie W, Huang X, Rusanen A, Ehn M, et al. (2018). Modelling studies of HOMs and their contributions to new particle formation and growth: comparison of boreal forest in Finland and a polluted environment in China. *Atmospheric Chemistry and Physics*, 18(16): 11779–11791
- Shang D J, Peng J F, Guo S, Wu Z J, Hu M (2021). Secondary aerosol formation in winter haze over the Beijing-Tianjin-Hebei region, China. *Frontiers of Environmental Science & Engineering*, 15(2): 34
- Shi X Q, Brasseur G P (2020). The response in air quality to the reduction of Chinese Economic activities during the COVID-19 outbreak. *Geophysical Research Letters*, 47(11): 2020GL088070
- Shilling J E, Pekour M S, Fortner E C, Artaxo P, De Sa S, Hubbe J M, Longo K M, Machado L A T, Martin S T, Springston S R, et al. (2018). Aircraft observations of the chemical composition and aging of aerosol in the Manaus urban plume during GoAmazon 2014/5. *Atmospheric Chemistry and Physics*, 18(14): 10773–10797
- Shrivastava M, Andreae M O, Artaxo P, Barbosa H M J, Berg L K, Brito J, Ching J, Easter R C, Fan J W, Fast J D, et al. (2019). Urban pollution greatly enhances formation of natural aerosols over the Amazon rainforest. *Nature Communications*, 10(1): 1046
- Stein A F, Draxler R R, Rolph G D, Stunder B J B, Cohen M D, Ngan F (2015). NOAA's hysplit atmospheric transport and dispersion modeling system. *Bulletin of the American Meteorological Society*, 96(12): 2059–2077
- Sun P, Nie W, Wang T, Chi X, Huang X, Xu Z, Zhu C, Wang L, Qi X, Zhang Q, et al. (2020a). Impact of air transport and secondary formation on haze pollution in the Yangtze River Delta: *in situ* online observations in Shanghai and Nanjing. *Atmospheric Environment*, 225: 117350
- Sun Y L, Lei L, Zhou W, Chen C, He Y, Sun J X, Li Z J, Xu W Q, Wang Q Q, Ji D S, et al. (2020b). A chemical cocktail during the COVID-19 outbreak in Beijing, China: insights from six-year aerosol particle composition measurements during the Chinese New Year holiday. *Science of the Total Environment*, 742: 140739
- Turpin B J, Huntzicker J J (1995). Identification of secondary organic aerosol episodes and quantitation of primary and secondary organic aerosol concentrations during scaqs. *Atmospheric Environment*, 29(23): 3527–3544
- Ulbrich I M, Canagaratna M R, Zhang Q, Worsnop D R, Jimenez J L (2009). Interpretation of organic components from Positive Matrix Factorization of aerosol mass spectrometric data. *Atmospheric Chemistry and Physics*, 9(9): 2891–2918
- Virkkula A, Chi X, Ding A, Shen Y, Nie W, Qi X, Zheng L, Huang X, Xie Y, Wang J, et al. (2015). On the interpretation of the loading correction of the aethalometer. *Atmospheric Measurement Techniques*, 8(10): 4415–4427
- Wang H L, An J L, Shen L J, Zhu B, Pan C, Liu Z R, Liu X H, Duan Q, Liu X, Wang Y S (2014). Mechanism for the formation and microphysical characteristics of submicron aerosol during heavy haze pollution episode in the Yangtze River Delta, China. *Science of the Total Environment*, 490: 501–508
- Wang J, Nie W, Cheng Y, Shen Y, Chi X, Wang J, Huang X, Xie Y, Sun P, Xu Z, et al. (2018). Light absorption of brown carbon in eastern China based on 3-year multi-wavelength aerosol optical property observations and an improved absorption Angstrom exponent segregation method. *Atmospheric Chemistry and Physics*, 18(12): 9061–9074
- Wang J F, Ge X L, Chen Y F, Shen Y F, Zhang Q, Sun Y L, Xu J Z, Ge S, Yu H, Chen M D (2016). Highly time-resolved urban aerosol characteristics during springtime in Yangtze River Delta, China: insights from soot particle aerosol mass spectrometry. *Atmospheric Chemistry and Physics*, 16(14): 9109–9127
- Wang J F, Ge X L, Sonya C, Ye J H, Lei Y L, Chen M D, Zhang Q (2022a). Influence of regional emission controls on the chemical composition, sources, and size distributions of submicron aerosols: Insights from the 2014 Nanjing Youth Olympic Games. *Science of the Total Environment*, 807: 150869
- Wang J F, Liu D T, Ge X L, Wu Y Z, Shen F Z, Chen M D, Zhao J, Xie C H, Wang Q Q, Xu W Q, et al. (2019). Characterization of black carbon-containing fine particles in Beijing during wintertime. *Atmospheric Chemistry and Physics*, 19(1): 447–458
- Wang S Y, Zhao Y L, Han Y, Li R, Fu H B, Gao S, Duan Y S, Zhang L W, Chen J M (2022b). Spatiotemporal variation, source and secondary transformation potential of volatile organic compounds (VOCs) during the winter days in Shanghai, China. *Atmospheric Environment*, 286: 119203
- Wang Y Y, Li Z Q, Wang Q Y, Jin X A, Yan P, Cribb M, Li Y A, Yuan C, Wu H, Wu T, Ren R M, et al. (2021). Enhancement of secondary aerosol formation by reduced anthropogenic emissions during Spring Festival 2019 and enlightenment for regional PM_{2.5} control in Beijing. *Atmospheric Chemistry and Physics*, 21(2): 915–926
- Wu K, Kang P, Tie X, Gu S, Zhang X, Wen X, Kong L, Wang S, Chen Y, Pan W, et al. (2019). Evolution and assessment of the atmospheric composition in Hangzhou and its surrounding areas during the G20 summit. *Aerosol and Air Quality Research*, 9(12): 2757–2769
- Wu K, Yang X Y, Chen D, Gu S, Lu Y Q, Jiang Q, Wang K, Ou Y H, Qian Y, Shao P, et al. (2020). Estimation of biogenic VOC emissions and their corresponding impact on ozone and secondary organic aerosol formation in China. *Atmospheric Research*, 231: 104656
- Xu J X, Zhu F H, Wang S, Zhao X Y, Zhang M, Ge X L, Wang J F, Tian W X, Wang L W, Yang L, et al. (2019a). Impacts of relative humidity on fine aerosol properties via environmental wind tunnel experiments. *Atmospheric Environment*, 206: 21–29
- Xu L, Du L, Tsona N T, Ge M F (2021). Anthropogenic effects on biogenic secondary organic aerosol formation. *Advances in Atmospheric Sciences*, 38(7): 1053–1084
- Xu L, Guo H Y, Boyd C M, Klein M, Bougiatioti A, Cerully K M, Hite J R, Isaacman-Vanwertz G, Kreisberg N M, Knote C, et al. (2015). Effects of anthropogenic emissions on aerosol formation from isoprene and monoterpenes in the southeastern United States. *Proceedings of the National Academy of Sciences of the United States of America*, 112(1): 37–42

- Xu L, Lingaswamy A P, Zhang Y X, Liu L, Wang Y Y, Zhang J, Ma Q L, Li W J (2019b). Morphology, composition, and sources of individual aerosol particles at a regional background site of the YRD, China. *Journal of Environmental Sciences (China)*, 77: 354–362
- Xu W Q, Zhou W, Li Z J, Wang Q Q, Du A D, You B, Qi L, Prevot A S H, Cao J J, Wang Z F, et al. (2022). Changes in primary and secondary aerosols during a controlled Chinese New Year. *Environmental Pollution*, 315: 120408
- Xu Z N, Huang X, Nie W, Chi X G, Xu Z, Zheng L F, Sun P, Ding A J (2017). Influence of synoptic condition and holiday effects on VOCs and ozone production in the Yangtze River Delta region, China. *Atmospheric Environment*, 168: 112–124
- Yang L W, Nie W, Liu Y L, Xu Z N, Xiao M, Qi X M, Li Y Y, Wang R X, Zou J, Paasonen P, et al. (2021). Toward building a physical proxy for gas-phase sulfuric acid concentration based on its budget analysis in polluted Yangtze River Delta, east China. *Environmental Science & Technology*, 55(10): 6665–6676
- Yang Y, Wang Y H, Yao D, Zhao S M, Yang S H, Ji D S, Sun J, Wang Y H, Liu Z R, Hu B, et al. (2020). Significant decreases in the volatile organic compound concentration, atmospheric oxidation capacity and photochemical reactivity during the National Day holiday over a suburban site in the North China Plain. *Environmental Pollution*, 263: 114657
- Ye Z L, Liu J S, Gu A J, Feng F F, Liu Y H, Bi C L, Xu J Z, Li L, Chen H, Chen Y F, et al. (2017). Chemical characterization of fine particulate matter in Changzhou, China, and source apportionment with offline aerosol mass spectrometry. *Atmospheric Chemistry and Physics*, 17(4): 2573–2592
- Yu Y, Wang H, Wang T T, Song K, Tan T Y, Wan Z C, Gao Y Q, Dong H B, Chen S Y, Zeng L M, et al. (2021). Elucidating the importance of semi-volatile organic compounds to secondary organic aerosol formation at a regional site during the EXPLORE-YRD campaign. *Atmospheric Environment*, 246: 118043
- Zhang J K, Wang Y S, Huang X J, Liu Z R, Ji D S, Sun Y (2015a). Characterization of organic aerosols in Beijing using an aerodyne high-resolution aerosol mass spectrometer. *Advances in Atmospheric Sciences*, 32(6): 877–888
- Zhang Q, Geng G (2019). Impact of clean air action on PM_{2.5} pollution in China. *Science China. Earth Sciences*, 62(12): 1845–1846
- Zhang Q, Jimenez J L, Canagaratna M R, Ulbrich I M, Ng N L, Worsnop D R, Sun Y L (2011). Understanding atmospheric organic aerosols via factor analysis of aerosol mass spectrometry: a review. *Analytical and Bioanalytical Chemistry*, 401(10): 3045–3067
- Zhang Q, Worsnop D R, Canagaratna M R, Jimenez J L (2005). Hydrocarbon-like and oxygenated organic aerosols in Pittsburgh: insights into sources and processes of organic aerosols. *Atmospheric Chemistry and Physics*, 5(12): 3289–3311
- Zhang Q, Zheng Y X, Tong D, Shao M, Wang S X, Zhang Y H, Xu X D, Wang J N, He H, Liu W Q, et al. (2019). Drivers of improved PM_{2.5} air quality in China from 2013 to 2017. *Proceedings of the National Academy of Sciences of the United States of America*, 116(49): 24463–24469
- Zhang Y J, Tang L L, Wang Z, Yu H X, Sun Y L, Liu D, Qin W, Canonaco F, Prevot A S H, Zhang H L, et al. (2015b). Insights into characteristics, sources, and evolution of submicron aerosols during harvest seasons in the Yangtze River delta region, China. *Atmospheric Chemistry and Physics*, 15(3): 1331–1349
- Zhang Y J, Tang L L, Yu H X, Wang Z, Sun Y L, Qin W, Chen W T, Chen C H, Ding A J, Wu J, et al. (2015c). Chemical composition, sources and evolution processes of aerosol at an urban site in Yangtze River Delta, China during wintertime. *Atmospheric Environment*, 123: 339–349
- Zhang Y W, Zhang X Y, Zhang Y M, Shen X J, Sun J Y, Ma Q L, Yu X M, Zhu J L, Zhang L, Che H C (2015d). Significant concentration changes of chemical components of PM₁ in the Yangtze River Delta area of China and the implications for the formation mechanism of heavy haze-fog pollution. *Science of the Total Environment*, 538: 7–15
- Zhao D F, Pullinen I, Fuchs H, Schrade S, Wu R R, Acir I H, Tillmann R, Rohrer F, Wildt J, Guo Y D, et al. (2021). Highly oxygenated organic molecule (HOM) formation in the isoprene oxidation by NO₃ radical. *Atmospheric Chemistry and Physics*, 21(12): 9681–9704
- Zhao J, Du W, Zhang Y J, Wang Q Q, Chen C, Xu W Q, Han T T, Wang Y Y, Fu P Q, Wang Z F, et al. (2017). Insights into aerosol chemistry during the 2015 China Victory Day parade: results from simultaneous measurements at ground level and 260 m in Beijing. *Atmospheric Chemistry and Physics*, 17(4): 3215–3232
- Zhao Q B, Huo J T, Yang X, Fu Q Y, Duan Y S, Liu Y X, Lin Y F, Zhang Q (2020). Chemical characterization and source identification of submicron aerosols from a year-long real-time observation at a rural site of Shanghai using an Aerosol Chemical Speciation Monitor. *Atmospheric Research*, 246: 105154
- Zheng G J, Duan F K, Ma Y L, Zhang Q, Huang T, Kimoto T, Cheng Y F, Su H, He K B (2016). Episode-based evolution pattern analysis of haze pollution: method development and results from Beijing, China. *Environmental Science & Technology*, 50(9): 4632–4641
- Zhou M, Nie W, Qiao L, Huang D D, Zhu S, Lou S, Wang H, Wang Q, Tao S, Sun P, et al. (2022a). Elevated formation of particulate nitrate from N₂O₅ hydrolysis in the Yangtze River delta region from 2011 to 2019. *Geophysical Research Letters*, 49(9)
- Zhou W, Xu W Q, Wang Q Q, Li Y, Lei L, Yang Y, Zhang Z Q, Fu P Q, Wang Z F, Sun Y L (2022b). Machine learning elucidates the impact of short-term emission changes on air pollution in Beijing. *Atmospheric Environment*, 283: 119192